Journal of the Korean Nuclear Society
Volume 31, Number 1, pp.29~48, February 1999

Experimental Study on Two-Phase Flow Parameters of Subcoolet Boiling in Inclined Annulus

Tae-Ho Lee, Moon-Oh Kim and Goon-Cherl Park
Seoul National University,
Shinlim-Dong 56-1, Gwanak-Gu, Seoul 151-742, Korea.

(Received February 18, 1998)

Abstract

Local two-phase flow parameters of subcooled flow boiling in inclined annulus were measured to investigate the effect of inclination on the internal flow structure. Two-conductivity probe technique was applied to measure local gas phasic parameters, including void fraction, vapor bubble frequency, chord length, vapor bubble velocity and interfacial area concentration. Local liquid velocity was measured by Pitot tube. Experiments were conducted for three angles of inclination; 0° (vertical), 30°, 60°. The system pressure was maintained at atmospheric pressure. The range of average void fraction was up to 10% and the average liquid superficial velocities were less than 1.3 m/sec. The results of experiments showed that the distributions of two-phase flow parameters were influenced by the angle of channel inclination. Especially, the void fraction and chord length distributions were strongly affected by the increase of inclination angle, and flow pattern transition to slug flow was observed depending on the flow conditions. The profiles of vapor velocity, liquid velocity and interfacial area concentration were found to be affected by the non-symmetric bubble size distribution in inclined channel. Using the measured distributions of local phasic parameters, an analysis for predicting average void fraction was performed based on the drift flux model and flowing volumetric concentration. And it was demonstrated that the average void fraction can be more appropriately presented in terms of flowing volumetric concentration.

1. Introduction

In a wide variety of engineering systems, two-phase flow has been the subject of numerous investigations for their optimum design and safe operation. Some of the important applications include transportations of two-phase mixture in pipelines, nuclear reactor systems, refrigeration

Key Words : flow boiling, inclination, two-conductivity probe, pitot tube, void fraction, vapor bubble frequency, vapor bubble velocity, interfacial area concentration, chord length, liquid velocity, drift flux parameters, flowing volumetric concentration

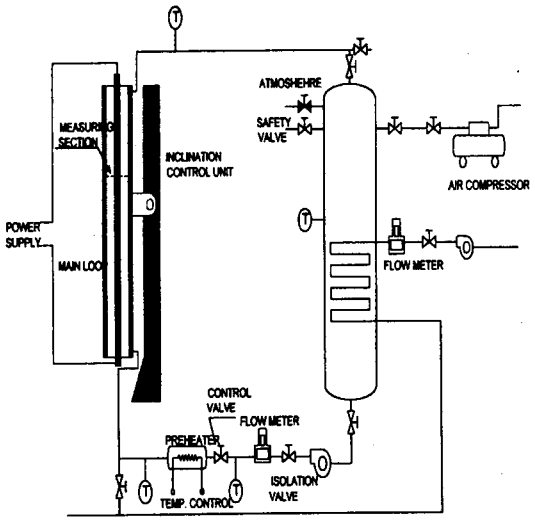

Fig. 1. Schematics of Experimental Facility

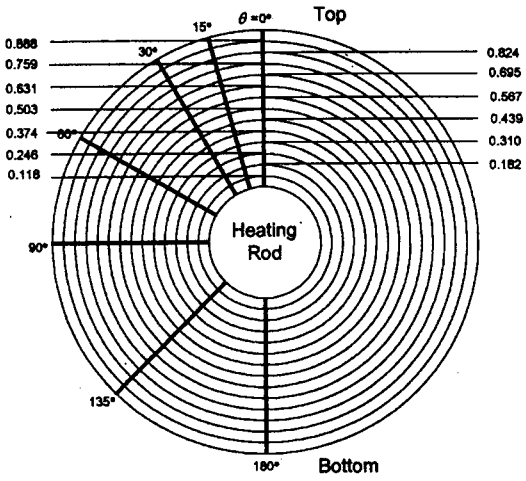

Fig. 2. Probe Positions in Inclined Channel

systems, operations of evaporators, etc. In order to improve the efficiency and to analyze the safety of such systems, it is important to know the detailed internal structure of two-phase flow. Although extensive studies on two-phase flow phenomena have been made, most of these works have been done in vertical conduits. So, works on two-phase flow in inclined channel are limited so far. Moreover, most of the work has been made in the adiabatic two phase flow condition (Barnea et al.[1,2], Weisman and Kang[3], Spedding et al[4], Stanislav et al.[5], Spindler[6]).

Spindler[6] measured the local void fraction and bubble frequency using the fiber optical probe in inclined pipes, and showed that the radial distribution of local void fraction and bubble frequency in inclined two-phase flow was strongly influenced by the angle of inclination. However, this work was limited to adiabatic air-water two-phase flow. On the other hand, Fedorov and Klimenko[7] found from the experimental study on flow boiling that the local heat transfer coefficient depended on the orientation of the channel. The heat transfer coefficient in the upper circumference of the channel showed somewhat weaker dependency on the heat flux than in the lower circumference. This effect is obviously connected to the non-symmetry of the two-phase flow structure. So, more comprehensive understanding on the two-phase flow phenomena needs to predict the two-phase flow structure by local measurements on flow boiling in inclined channel. However, the works on the local measurements of two-phase flow parameters in inclined boiling channel are extremely lacked. The mechanism of boiling heat transfer in inclined channel is closely related to the distributions of the liquid and vapor phases. Therefore, for identifying the heat transfer phenomena in the inclinable systems such as ship reactor and absorber tube of a concentrating parabolic through collector with direct steam generation, it is necessary to know the local flow conditions at different angles of inclination in flow boiling.

The present study has mainly focused on the experimental investigation of local two-phase flow parameters in inclined subcooled boiling annulus under the atmospheric pressure. Local void

Table 1. Experimental Conditions

Inclination	<α>	<j_L>	<j_G>	Inclination	<α>	<j_L>	<j_G>
0° (vertical)	0.0948	0.6893	0.1030	30°	0.0174	0.8776	0.0159
	0.0280	0.7403	0.0268		0.0232	0.9008	0.0249
	0.0514	0.7456	0.0539		0.0556	0.8924	0.0699
	0.0606	0.7361	0.0643		0.0289	1.0847	0.0364
	0.0400	0.7964	0.0420		0.0409	1.0426	0.0581
	0.0413	0.7901	0.0431		0.0669	1.0704	0.1021
	0.0097	0.9219	0.0094		0.0880	1.0442	0.1415
	0.0342	0.9164	0.0400		0.0103	1.2846	0.0127
	0.0418	0.9071	0.0504		0.0315	1.2617	0.0458
	0.0472	0.9302	0.0572		0.0431	1.2590	0.0662
	0.0677	0.9128	0.0871	60°	0.0258	0.9639	0.0268
	0.0899	0.9282	0.1240		0.0444	0.9234	0.0533
	0.0166	1.1095	0.0162		0.0708	0.9371	0.0857
	0.0337	1.0903	0.0359		0.0993	0.9220	0.1356
	0.0457	1.1082	0.0532		0.0182	1.1063	0.0210
	0.0719	1.0801	0.0886		0.0361	1.0745	0.0432
	0.0856	1.0670	0.1121		0.0365	1.0788	0.0481
					0.0870	1.0406	0.1253
					0.0094	1.2747	0.0104
					0.0343	1.2421	0.0470
					0.0600	1.2112	0.0874

fraction, vapor bubble frequency, chord length, vapor bubble velocity and interfacial area concentration (IAC) have been measured by using the two-conductivity probe. Also the local liquid velocity was measured by Pitot tube. Using the experimental results, an analysis for modeling the average void fraction was conducted based on the drift flux model and flowing volumetric concentration.

2. Experimental Facility and Procedure

Experimental facility is illustrated in Figure 1. The test loop basically consists of a test channel, a cooler, a pump and a preheater. The test channel is a concentric annular type, that is, a heating rod of 19 mm O.D. is placed in the center of a circular stainless steel tube of 37.5 mm I.D. The entire test channel is 2.3 m long and the angle of inclination can be adjusted between 0° (vertical) and 90° (horizontal). The heating rod is electrically heated and has a maximum power of 30 kW. The measuring section is located about 1.6 m downstream of the test channel inlet (L/D_h=87). The transparent glass tube of 50 mm long is installed in the measuring section, so that flow visualization with high-speed photography is possible. In order to investigate the variations of local two-phase flow parameters over the entire cross section, the measuring section is designed to be rotated by 360°. Traversing units, composed of ball slide units and micro vernier meters with 1/100 spatial resolution, are used to traverse the local probes in a direction perpendicular to the axis of the test channel. Distilled water is used as working fluid and its flow rate entering the test

channel is measured by turbine flow meter. The absolute pressure transducer is located in the measuring section, and T-type thermocouples are installed in the measuring section, channel inlet and outlet. The inlet liquid temperature is controlled by a preheater.

Experiments were carried out under the subcooled boiling by varying heat flux, inlet subcooling, inlet liquid flow rate and channel inclination. Inlet subcoolings and heat fluxes were adjusted at 6.6 ℃ $\leq \Delta T_{sub} \leq$ =18.3℃ and 69 kW/m^2 $\leq q'' \leq$ 278 kW/m^2, respectively, to obtain the desired area averaged void fractions for a given inlet liquid flow rate. Three angles of inclination (0°, 30°, 60°) were selected, and the system pressure was maintained at atmospheric pressure. A total of 38 experimental sets was carried out. A summary of the experimental conditions is described in Table 1. Measuring positions for vertical channel have been chosen as 13 points along the radial direction, assuming the symmetry of flow. For inclined channels, the probes were traced at 91 selected points as illustrated in Figure 2. Additionally, the high speed photography using the digital video camera with maximum shutter speed of 1/4,000 sec was applied to visualize overall flow structure.

3. Measuring Methods

3.1. Two-Conductivity Probe Method

In this study, local vapor phasic parameters such as void fraction, chord length, vapor bubble velocity, vapor bubble frequency and IAC have been measured by the two-conductivity probe method. The conductivity probe method is based on the difference of electrical resistance between vapor and liquid phases. Although the probe method perturb the flow field, it has a merit for the local measurements of vapor phase

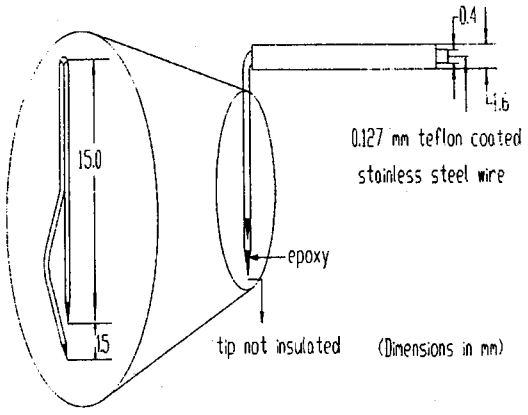

Fig. 3. Schematic Diagram of the Two-Conductivity Probe

parameters for a wide range of void fraction. Especially, in view of local measurements in inclined subcooled boiling with local void fractions ranging up to 65%, the probe method is considered to be the best choice. The concept of conductivity probe method was first proposed by Neal & Bankoff[8]. After that Serizawa et al.[9] and Welle[10] extended it to a two-conductivity probe method for measuring local gas phase parameters in vertical air-water flow. Also, Kocamustafaogullari & Wang[11] applied two-conductivity probe method to the measurements of local interfacial parameters in horizontal air-water bubbly flow, and recently Yun et al.[12] used it for measurements of local vapor parameters in the subcooled boiling.

The two-conductivity probe used in this study is schematically shown in Figure 3. The sensing elements of two probes are made of teflon-coated stainless steel wires with a diameter of 0.127 mm. Two probe tips are sharpened to form a conical shape and are aligned in the channel axial direction. The distance between two probe tips is adjusted to approximately 1.5 mm in the length wise direction.

3.1.1. Measurements of Local Void Fraction and Bubble Velocity

Instantaneous changes in local resistivities sensed by the two-conductivity probe are converted into a voltage drop between a probe tip and the ground by electrical circuit. Ideally, the voltage signals is the two-state square-wave signal. However, the signals generally deviate from the ideal signal form. This deviation is largely due to the finite size of the sensor and the possible deformation of the vapor bubble interface before the sensor enters one phase from the other. Thus, the cutoff level for the phase discrimination criterion has to be precisely determined to obtain accurate local void fraction and vapor bubble velocity.

For the phase discrimination in this study, the cutoff level calculation algorithm developed by Yun et al.[12] was adopted. The cutoff level is calculated based on the pulse height and slope criterion for each bubble, but the proportional constant for determining pulse height should be determined by experiments. In this study, this constant was determined by air-water experiments in the transparent pipe of 23 mm I.D. and 2,100 mm long. Experiments were conducted for four angles of inclination; 0°, 30°, 45°, 60°. The local void fractions were measured by using various proportional constants of 0.1SIM 0.9, and cross sectional averaged values were compared with the average void fraction by the quick closing valve technique. The optimum proportional constant was determined to be 0.35. Figure 4 shows the comparison of average void fraction by the quick closing valve technique and that by probe. The mean deviation were found to be bold ±2.5 % and thus the proportional constant of 0.35 was found to be resonable for all channel inclination angle.

Although the local void fraction can be obtained

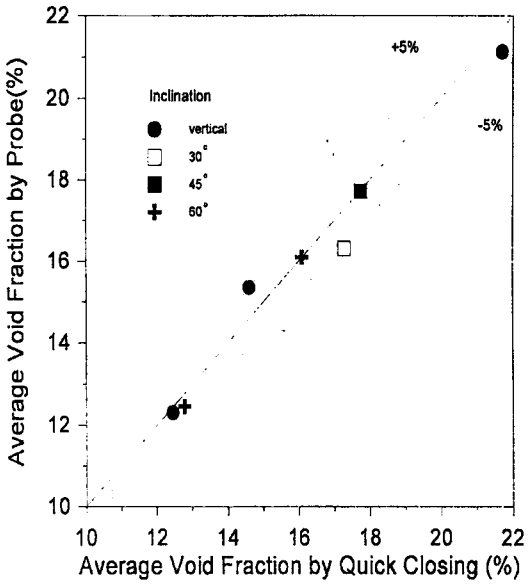

Fig. 4. Comparison Between Average Void Fraction Measured by Probe and Quick Closing

independently with both front and rear probe, the void fraction was determined by front probe because the signal from rear probe could be affected by the wake of a vapor that has passed the front probe. The local vapor bubble frequency, which is the number of vapor bubbles detected in unit time at a specific location, was also measured at front probe.

The local vapor bubble velocity can be determined from the two processed signals of two-conductivity probe. If a vapor which is in contact with the front probe subsequently makes contact with the rear probe, the time delay between the contact signals is a measure of the vapor velocity. The vapor bubble velocity component in the axial direction can be expressed as follows;

$$V_g = \frac{\Delta z}{\Delta t} \tag{1}$$

where Δt is time delay and Δz is the distance

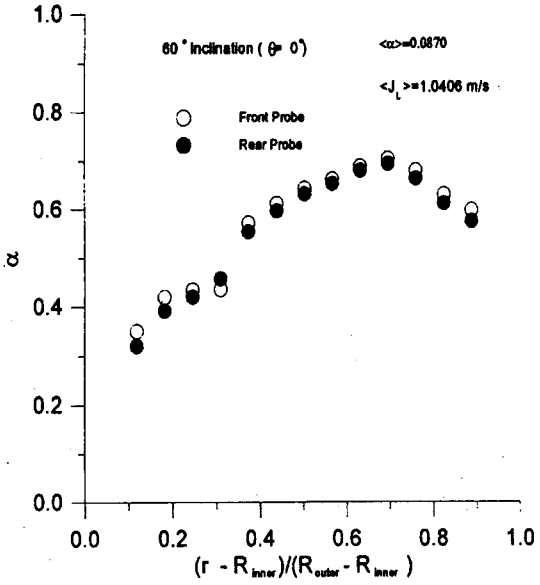

Fig. 5. Typical Void Fraction Measured by Front and Rear Probes

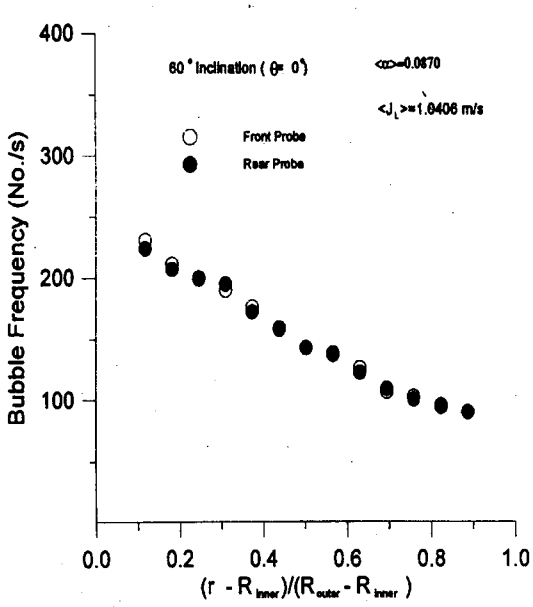

Fig. 6. Typical Void Fraction Measured by Front and Rear Probes

between two probe tips.

However, the two signals detected by the front and rear probes do not always correspond to the same vapor. Thus, the signal validation is necessary for judging whether the signals from both probes originates from the same vapor. In this work, this validation was performed by comparing the vapor resident times, time to take a vapor bubble to pass the probe, at the front and rear probes. If a difference of vapor resident times at the front and the rear probe is within bold ± 20 % compared with the vapor resident time at the front probe, then the two signals detected by both probes were considered to be originated from the same vapor. This method used in the determination of the time delay produces the local vapor bubble velocity spectrum. The local mean velocity was calculated from the spectrum.

The proper probe distance between two probe tips is critical for measuring the vapor bubble velocity with sufficient accuracy. If the distance is too small, inaccuracies in time duration measurements may be caused unless very high sampling frequency of A/D converter is supported. During the present experiments, a sampling rate of 60 kHz was used. On the other hand, if the distance is too large, a vapor bubble cut by the front probe may miss the rear probe, or bubbles, which do not pass the front probe, may cut in. Most previous investigators have used a distance of 5 mm in their vertical adiabatic flow experiments. On the other hand, Kocamustafaogullari and Wang[11] adopted the probe distance of 2.5 mm in horizontal air-water bubbly flow. However, more attention should be paid to determine the distance in case of flow boiling in inclined channel because vapors can generate on the heating surface in the space between two probe tips and bubbles grown up on the heating surface may have the lateral velocity components which are larger than those in vertical channel. Preliminary experiments in inclined boiling

channel showed that the probe distance of 5 mm or 2.5 mm was large for the present experiment since void fraction and vapor bubble frequency measured by rear probe is much higher than those by front probe. This fact required a smaller probe distance. In this study, from the analyses of high speed photography and some preliminary test results obtained by using the two-conductivity probes with different probe distances, it was decided that 1.5 mm was the appropriate distance for flow boiling experiment in inclined channel. Figures 5 and 6 show typical distributions of void fraction and vapor bubble frequency, respectively, which are measured by the front and rear probes with a probe distance of 1.5 mm. The local void fractions and vapor bubble frequencies obtained at two probes coincides well with each other.

For the verification of the vapor bubble velocity measured by two-conductivity probe, separate air/water experiments in a transparent tube, into which porous stick was inserted, have been carried out. The local velocity of a bubble ejected out of holes on the porous stick was measured by two-conductivity probe and compared with that measured simultaneously by high speed photography. The high speed camera(PHOTEC), whose maximum shutter speed is 10,000 frames/sec, was used, and the shutter speed was set to 2,000 frames/sec. Experiments were conducted for three angles of inclination; 0°, 45°, 90°. Figure 7 shows the comparison of local vapor bubble velocities measured by two-conductivity probe and high speed photography. The comparison showed good agreement and the mean deviation was bold ±3.3 %.

The local vapor bubble chord length can be determined from the product of the vapor bubble resident time and vapor velocity, and be considered as a measure of vapor bubble size. The local mean chord length was calculated from the local mean vapor velocity and the vapor resident

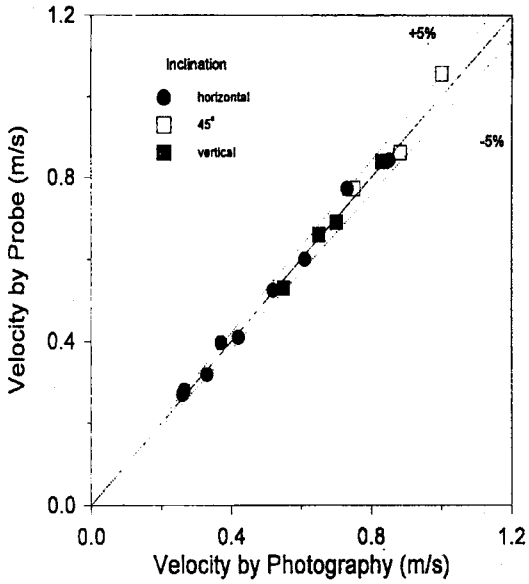

Fig. 7. Comparison Between Local Vapor Bubble Velocity by Probe and Photography

time spectrum measured by the front probe.

3.1.2. Measurement of Local Interfacial Area Concentration

In predicting two-phase flow phenomena using the two-fluid model formulation, the interfacial transfer terms are essential factors in the modeling. The interfacial transfer terms specify the rate of phase change, momentum transfer and heat transfer at the interface between phases, and those are strongly related to the interfacial area and to the local transfer mechanism. Basically, the interfacial transport of mass, momentum and energy is proportional to the IAC and driving force. Thus, the knowledge of the IAC is indispensible in the two-fluid model. Since the IAC can not be treated as a variable to be solved from a set of balance equations, it should be specified by a constitutive relation or by introducing an additional transport equation for it.

The local IAC at any spatial point r is given by Ishii[13] as;

$$a_i(r) = \frac{1}{T} \sum_{j=1}^{N_t} \frac{1}{| v_i \cdot n_i |_j} \quad (2)$$

where T, v_i and n_i are the sampling time, bubble interface velocity and surface unit normal vector of j-th interface. N_t is the total number of interfaces passing through the point within the sampling time. Physically this local IAC represents the probability of the interface occurring at that point and can be measured through Eq.(2) using four-sensors method proposed by Kataoka et al.[14]. However, application of four-sensors method is limited to relatively large bubbles and large diameter channel due to its complex geometry. They also suggested a practical measuring method to obtain local IAC by two-sensors(two-conductivity probe) method. They related the local IAC to locally measurable quantities associated with the bubble interface velocity under several statistical assumptions on bubble motion and simple geometric considerations. In this method, it is assumed that the bubbles are spherical and every part of the bubble has the same probability of being intersected by the probe. Then, the local IAC is given by;

$$a_i(r) = \frac{4N_t \left(\sum_j \frac{1}{|v_{szj}|} / (\sum_j) \right)}{1 - \cot\frac{\alpha_o}{2} \ln(\cos\frac{\alpha_o}{2}) - \tan\frac{\alpha_o}{2} \ln(\sin\frac{\alpha_o}{2})} \quad (3)$$

where v_{szj} is the velocity of j-th bubble measured by two-conductivity probe and α_o denotes the angle between the bubble velocity and the mean flow direction. With the assumption that the direction of the bubble velocity fluctuates within a maximum angle of α_o from the mean flow direction with equal probability, α_o is given by;

$$\frac{\sin 2\alpha_o}{2\alpha_o} = \frac{1 - (\sigma_z^2 / |\overline{v_{sz}}|^2)}{1 + 3(\sigma_z^2 / |\overline{v_{sz}}|^2)} \quad (4)$$

$$\sigma_z = \left(\sum_j N_{szj} (v_{szj} - \overline{v_{sz}})^2 / \sum_j N_{szj} \right)^{1/2} \quad (5)$$

In Eqs. (4) and (5), N_{szj} is the number of bubbles having the velocity of v_{szj} and $\overline{v_{szj}}$ is mean velocity. Using Eqs. (3), (4) and (5), the local IAC can be estimated by measuring the local vapor bubble velocity spectrum and bubble frequency at each measuring point. This method has been extensively used by several investigators such as Kataoka and Serizawa[15] for vertical adiabatic bubbly flow, Kocamustafaogullari and Wang[11] for horizontal air-water bubbly flow and Yun et al.[12] for subcooled boiling flow in vertical channel.

Kataoka et al.[16] investigated the effects of probe spacing, bubble diameter and hitting angle of bubbles on the accuracy of the local IAC measured by conductivity probes through the numerical simulation of a bubble passing the probes. They demonstrated that the two-conductivity probe method could be applied to a wide range of probe spacing and bubble diameter if the assumption that the probe passes every part of the bubble with equal probability is valid and the number of escaped bubbles before making contact with the rear probe is small. Particularly for small bubbles, the two-conductivity probe method was shown to be more accurate than the four-sensors method. In this study, two-conductivity probe method is used to determine the local IAC because the number of escaped bubbles is small as typically shown in Figure 6 and bubble sizes are relatively small except for near the upper end of the measuring section in inclined subcooled boiling channel.

Table 2. Data Reduction Models for Liquid Velocity by Pitot Tube (Reimann et al. 1983)

Adoni (1961)	:	$V_L=\frac{1}{\sqrt{(1-\alpha^2)}}\sqrt{\frac{2\Delta p}{\rho_L}}$
Neal & Bankoff (1965)	:	$V_L=\frac{1}{\sqrt{(1-\alpha)}}\sqrt{\frac{2\Delta p}{\rho_L}}$
Malnes (1966)	:	$V_L=\frac{1}{\sqrt{2(1-\alpha)}}\sqrt{\frac{2\Delta p}{\rho_L}}$
Walmet & Staub (1969)	:	$V_L=\frac{1}{\sqrt{(1-\alpha)(1+\alpha/2)}}\sqrt{\frac{2\Delta p}{\rho_L}}$
Delhaye & Chevrier (1969)	:	$V_L=\sqrt{\frac{2\Delta p}{\rho_L}}$
Bosio & Malnes (1969)	:	$V_L=\frac{1}{\sqrt{(1-\alpha^2/2)}}\sqrt{\frac{2\Delta p}{\rho_L}}$

3.2. Pitot Tube Method

The local liquid velocity was measured by Pitot tube. The local liquid velocity can be obtained by measuring the dynamic pressure which is the difference between the stagnation pressure and static pressure at the tube. The Pitot tube method has been widely used in the local measurements of air or liquid velocity. Although most applications were limited to single phase flow condition, some investigators applied this method to two-phase flow, and suggested models to calculated the local liquid velocity. The liquid velocity calculation models suggested by them are summarized in Table 2. (see Reimann et al.[17])

The problem encountered when using Pitot tube in two-phase flow are such that bubbles may flow into the Pitot tube and the flow field may be disturbed by the probe. In this study, a 1/16" Pitot tube (United Sensor) was used, and the dynamic pressure was measured by a diaphragm exchangeable type differential pressure transducer (Validyne DP103 with CD15 demodulator). These instruments minimize the possibilities of the problems cited above.

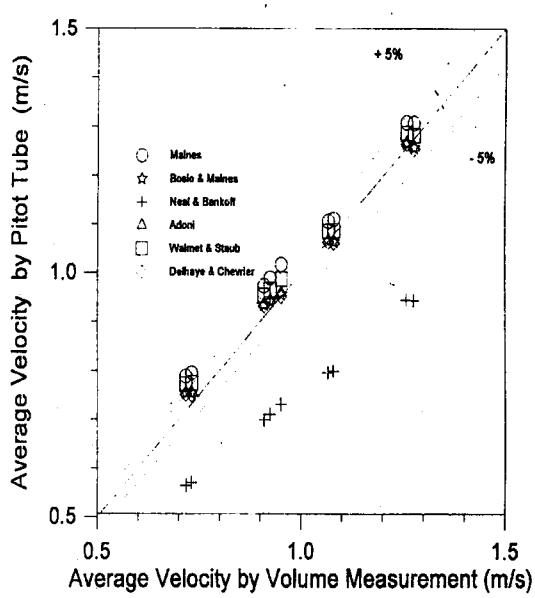

Fig. 8. Comparison Between Average Liquid Velocities by Pitot Tube and Volume Measurement

Air-water experiments were conducted for selecting the local liquid velocity calculation model

among the models listed in Table 2. The local liquid velocities were measured using the various models, and then the area averaged values of the measured local liquid velocities were compared with the average liquid velocity obtained by volume measurements. As can be seen in Figure 8, Delhaye & Chevrier and Bosio & Malnes models show good agreements. In this study, Delhaye & Chevrier model which has a minimum mean deviation of bold$\pm$1.75% among the models was selected for the local liquid velocity calculation.

4. Experimental Results and Discussion

4.1. Distribution of Local Void Fraction

The void fraction is one of the fundamental parameters which characterizes the structure of flow boiling because it reflects the energy of fluid and its distribution affects the distribution of other local parameters. The typical radial profiles of local void fraction are shown in Figure 9 for three angles of inclination. For inclined channels, radial profiles at θ=0° and 90° are presented.

For vertical channel, the local void fractions for all flow conditions decrease smoothly from the surface of heating rod to outerwall as shown in Figure 9. The maximum local void fraction is observed near the heating rod. These profiles of local void fraction are quite different from the so-called wall peaking of local void fraction reported for air-water two-phase flow by many investigators. The wall void peaking is known to be caused by the migration of bubbles toward the wall. The lift force plays a great role in the transverse migration of bubbles. Even though the nature of lift force is not fully understood yet, it is postulated so far to be generated by a bubble rotation and shear field in the continuous phase. However, in flow boiling, high values of local void fraction near the heating rod is due to the existence of heat source where the fluid enthalpy is high. The void fraction distribution in vertical boiling channel depends on the energy distribution in the subcooled boiling.

For inclined channels, the migration of vapor bubbles toward the upper part of the measuring section can be seen irrespective of flow conditions as shown in Figure 9, which yields non-symmetric void fraction profiles about channel axis. The local void fractions distribute across the measuring section in different ways depending on the area averaged void fraction and channel inclination, as following. For low area averaged void fractions less than about 3%, the maximum value of local void fraction is observed near the heating rod at θ =0°. However, for area averaged void fractions of 3~5 %, the void fraction distribution is influenced by the channel inclination. As shown typically in Figure 9, the position of maximum void fraction in 30° inclined channel is located near the heating rod. But, for 60° inclined channel, the location of maximum void fraction moves toward the channel center at θ=0°. This observation implies that the increase of channel inclination intensifies the asymmetry of the two-phase flow structure. For high area averaged void fractions more than about 5%, the local maximum void fraction is observed between channel center and outer wall at θ=0°. These non-symmetric void fraction distributions were confirmed by photographic study for visualizing overall flow structure, and the typical results are shown in Figure 10.

Spindler[6] observed that, as vertical tube inclined from vertical to horizontal, the air-water bubbly flow pattern disappeared because of high concentrations of voids at upper pipe crown. This fact supports that the buoyancy effect due to channel inclination is the most important parameter which determines the internal flow structure of two-phase flow in inclined channel.

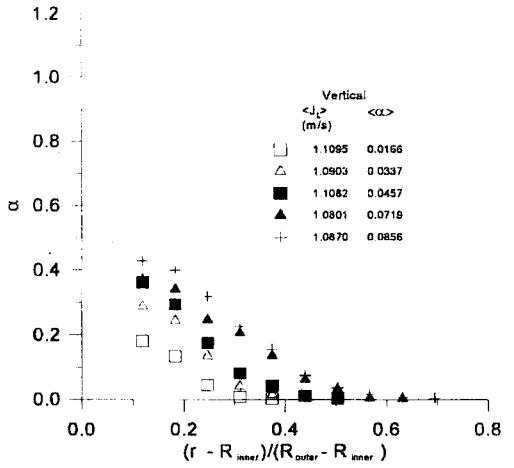

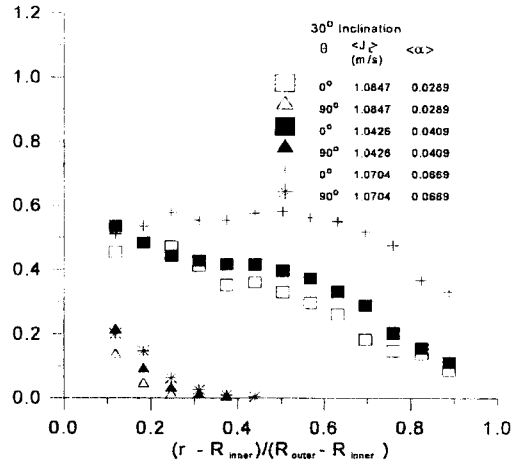

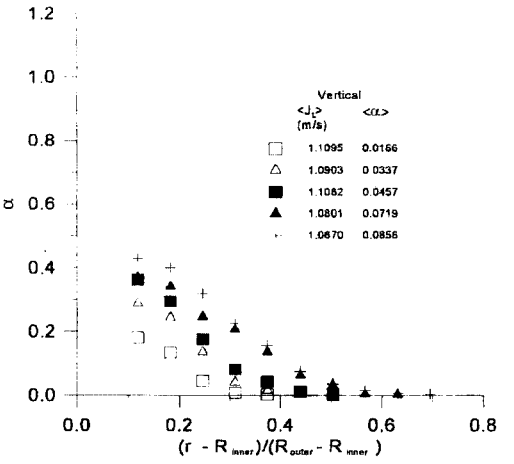

Fig. 9. Void Fraction Distributions

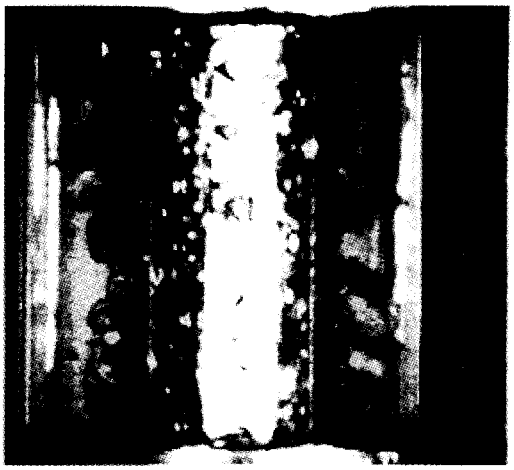

<α> ≃ 10%, Vertical>

< α> ≃ 10%, Inclination >

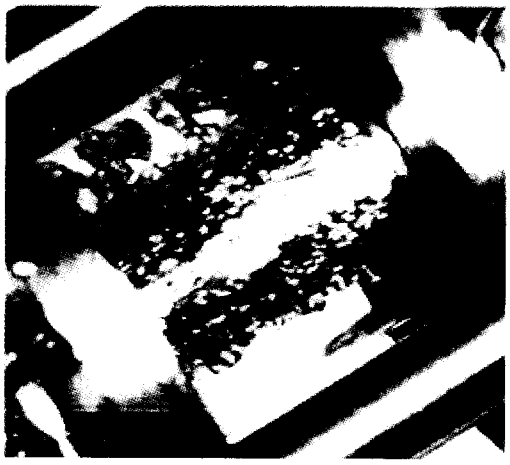

< α> ≃ 9%, 60° Inclination >

Fig. 10. Photographs of Overall Phase Distribution

4.2. Distributions of Local Vapor Bubble Frequency and Chord Length

Figures 11 and 12 describe the vapor bubble frequency and chord length profiles for the corresponding flow conditions of Figure 9. For vertical channel, the vapor bubble frequency profile very closely follows the void fraction distribution, but the distribution of chord length as a measure of vapor bubble size is nearly uniform. This means that the increase of local void fraction is not due to the increase of vapor bubble size but mainly due to the increase of vapor bubble frequency for a given flow condition in vertical channel.

For inclined channels, the local vapor bubble frequencies in the upper part of the measuring section are higher than those in the lower part, and the local chord length increases as moving from lower part of cross section to upper part at a given radial position. These observations imply explicitly that a number of vapor bubbles migrate toward the upper part of the test section by buoyancy, and bubble size increases by the bubble coalescence due to the high vapor bubble population in the upper cross section. Moreover, it can be noted from Figure 12 that flow pattern changes to slug flow in the upper part of cross section because the local chord length at θ=0° is larger than the channel gap size. As can be seen in Figures 9 and 12, high local void fraction at the upper part of cross section is caused by large bubble size in inclined channels, and this tendency becomes stronger as the channel inclination increases.

4.3. Distribution of Local Phasic Velocity

The typical radial profiles of the axial components of local vapor bubble velocities are illustrated in Figure 13. For vertical channel, the

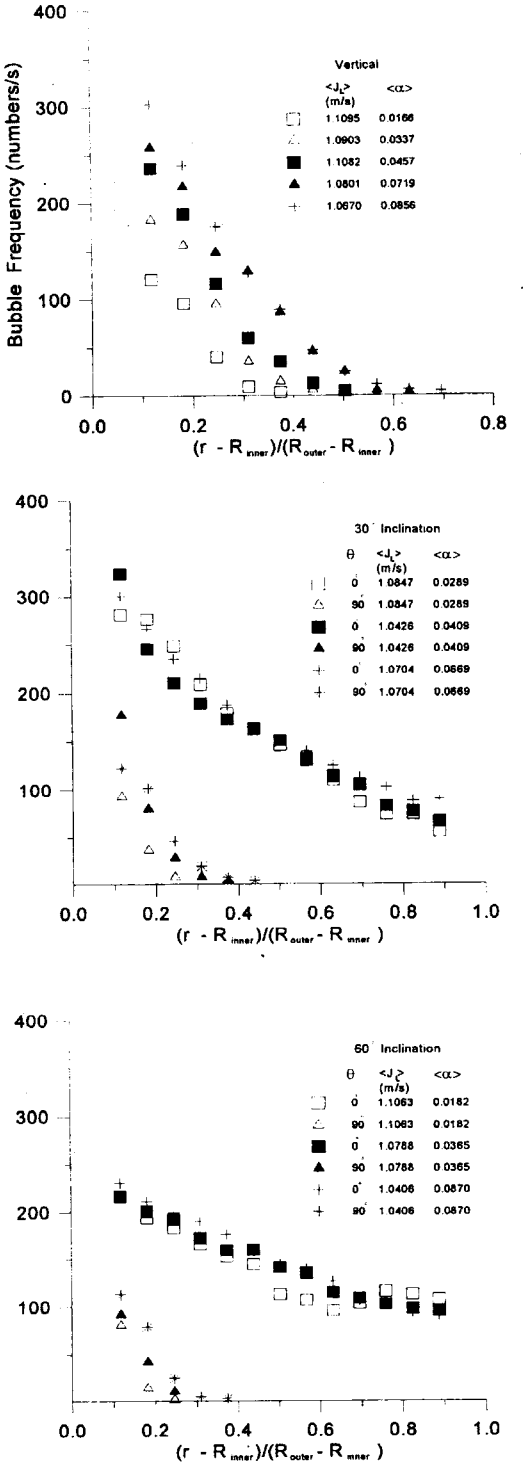

Fig. 11. Vapor Bubble Frequency Distributions

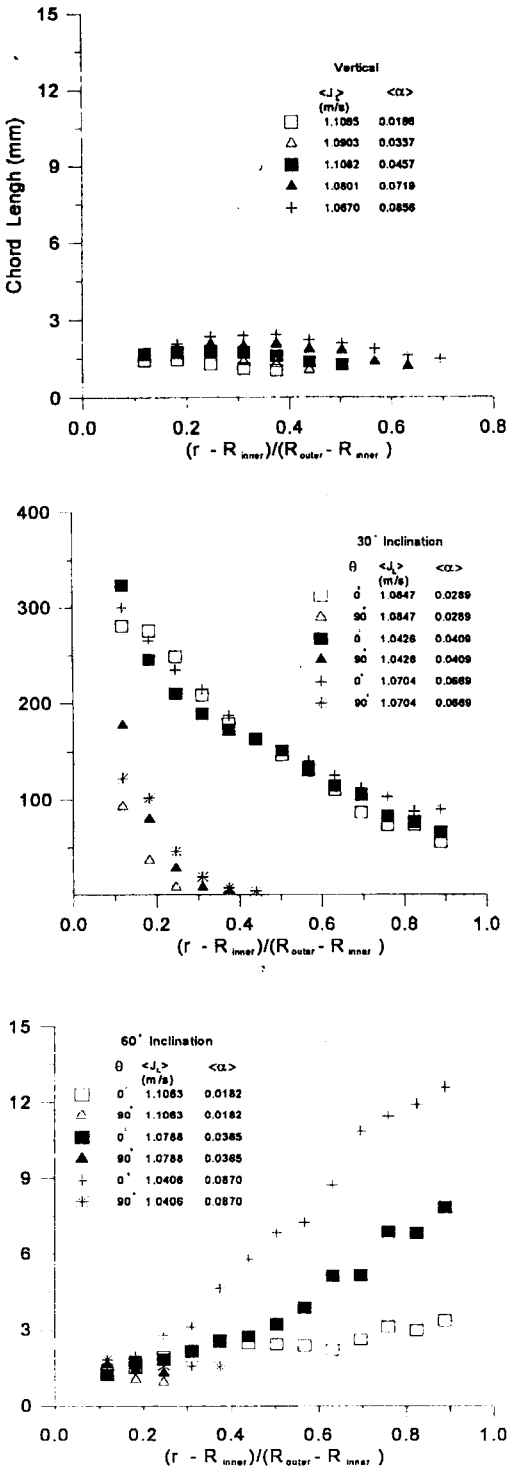

Fig. 12. Chord Length Distributions

local vapor bubble velocity increases from the heating surface to the channel center for all flow conditions. And the changes in the velocity profile shape are quite small compared with changes in the void fraction and vapor bubble frequency profiles. For inclined channels, the vapor velocity profile is also non-symmetric about channel axis as shown in the figure. The vapor velocity, in general, increases as moving toward the upper part of the cross section because of the buoyancy effect due to the increase of bubble size. However, the degree of non-symmetry of vapor velocity distribution is reduced as the liquid flow rate increases. For the average liquid superficial velocity above 1.21 m/sec, the effect of inclination on vapor velocity profile is mitigated.

Figure 14 show the typical profiles of local liquid velocities. In case of single-phase flow, the velocity profile is known to be parabolic along the radial direction due to the effect of shear force at the channel wall, irrespective of channel inclination. In case of two-phase flow, however, the nonuniformities of phase distribution and vapor bubble velocity across the cross section may cause the liquid velocity profile to deviate from that in single-phase liquid flow. As shown in the figure, the profiles of liquid velocity in vertical channel show the similar profiles to those in single-phase liquid flow. However, as the average liquid superficial velocity decreases below 0.8 m/sec, the location at which the maximum velocity of liquid phase occurs moves toward the heating rod. It is due to the fact that the vapor bubble with high velocity lifts the liquid phase with low velocity in low flow conditions. For inclined channels, the liquid velocity profile is also non-symmetric about channel axis. However, the liquid velocity profiles are more uniform than the vapor bubble velocity distributions. The local liquid velocities at θ=0° does not decrease from channel center to outer wall but increase generally from the surface of the

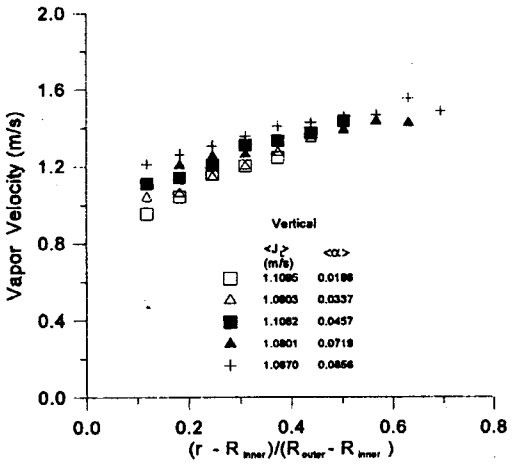

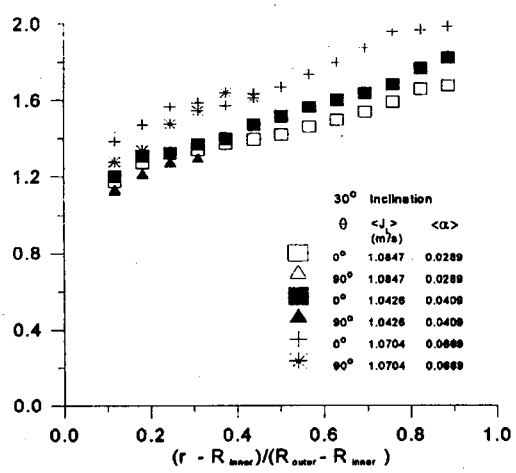

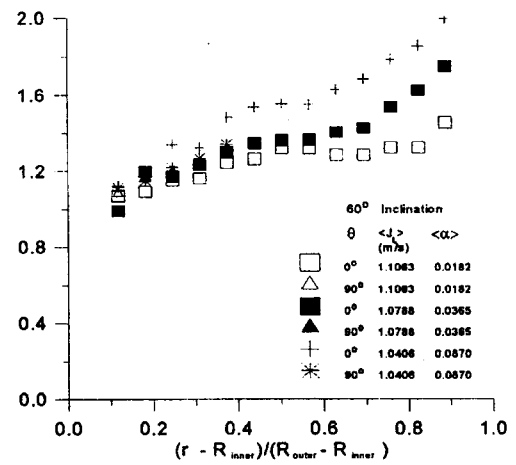

Fig. 13. Vapor Bubble Velocity Distributions

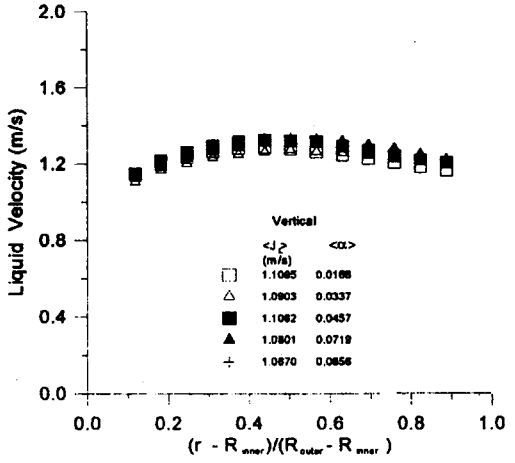

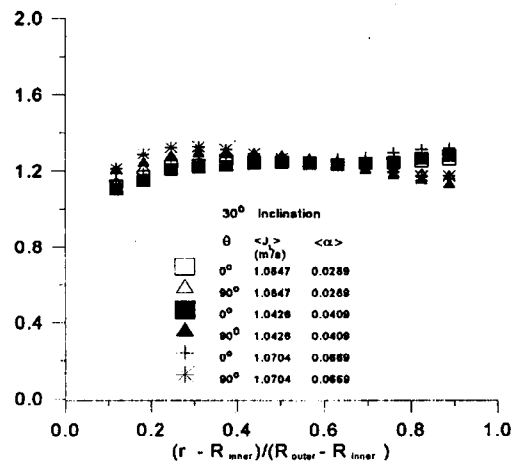

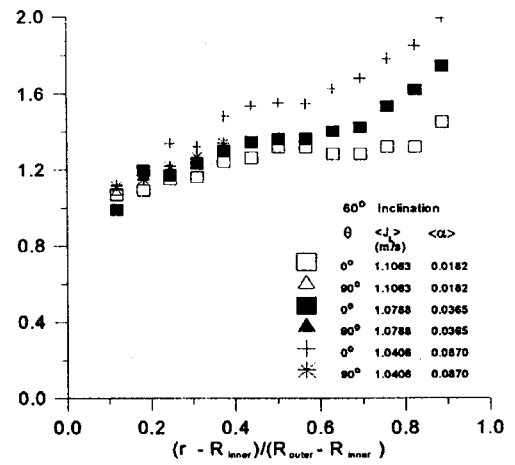

Fig. 14. Liquid Velocity Distributions

heating rod to outerwall. The reason for this observation is considered to be the lift by vapor bubbles having high velocity due to large bubble size between channel center and outer wall.

From Figures 13 and 14, it is interesting to note that the liquid velocity is faster than the vapor bubble velocity near the heating rod in some cases. Main reason for that observation comes from the fact that some bubbles around the heating rod does not have sufficient time to reach their terminal velocities. Moreover, for inclined channel, the velocity of the bubble detached from the boiling site have the velocity components other than axial direction, which are large compared to those in vertical channel.

4.4. Distributions of Local IAC

The typical local IAC profiles are described in Figure 15. For vertical channel, the radial distribution of local IAC has a trend similar to that of local void fraction. The profiles of the IAC and the void fraction can be used to determine the Sauter mean vapor bubble diameter variations along the measuring section. With the assumption that bubbles are spherically shaped, it can be shown that there exists a very simple relation among the local void fraction α, local IAC a_i and the local Sauter mean diameter d_{sm}, as follows;

$$a_i = \frac{6\alpha}{d_{sm}} \qquad (6)$$

Based on Eq. (6), typical Sauter mean diameter distributions are illustrated in Figure 16 for the corresponding flow conditions of Figure 15. From this figure it is observed that the Sauter mean vapor bubble size distribution for vertical channel is nearly uniform for a given flow condition. It is obvious from Eq.(6) that besides the void fraction, the bubble size also has a very important effect in determining the IAC, since the surface-to-volume

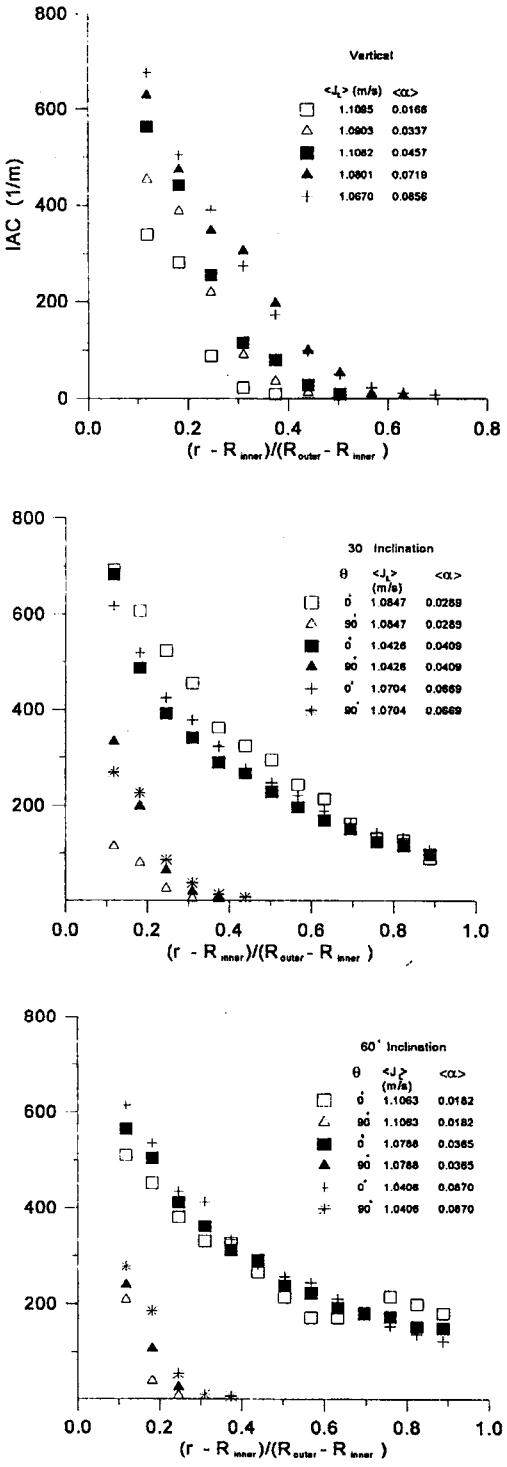

Fig. 15. IAC Distributions

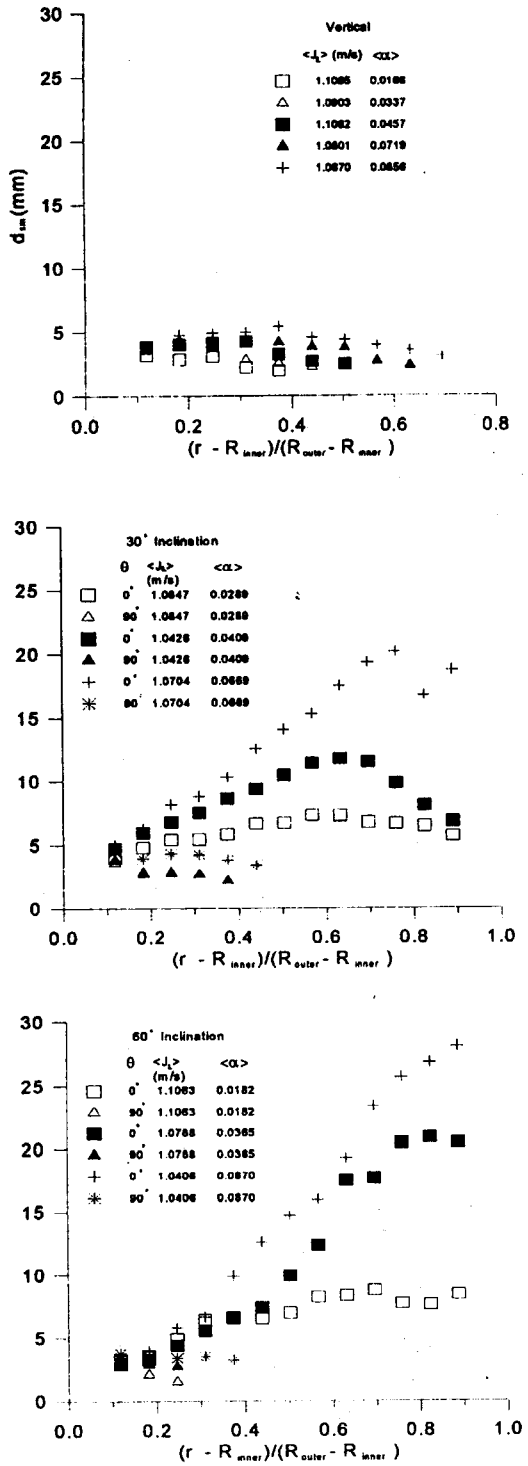

Fig. 16. Sauter Mean Diameter Distributions

ratio of a small bubble is larger than that of a larger bubble. However, considering small variations in the Sauter mean diameter, the observed similarity in profiles of the void fraction and IAC can be easily expected. As discussed previously, the increase of local void fraction in vertical channel is due to the increase of vapor bubble frequency. So, the most dominant reason for the increase of local IAC is the increase of local bubble frequency for a given flow condition.

For inclined channels, The IAC profiles very closely follow the vapor bubble frequency distributions. However the IAC profiles at upper part of cross section does not always show similar trend to the void fraction profiles as typically shown in Figures 9 and 15. Since the Sauter mean diameter distributions are highly nonuniform at the upper part of cross section as shown in Figure 16, it can be noted from Eq. (6) that the profiles of IAC is different from those of void fraction. Moreover, high local void fraction between channel center and outer wall at θ=0° is caused by local large bubble size as pointed out previously. So, it can be concluded that the IAC distribution in inclined channels is affected by bubble size distribution. The local IAC at the upper part is much higher than that at the lower part as shown in Figure 15. Since the local transports of mass, momentum and energy are directly proportional to the IAC, the figure points to the fact of a highly non-symmetric interfacial transport in inclined subcooled flow boiling.

4.5. Modeling of Average Void Fraction

Using the measured distributions of void fraction and velocity of each phase, the average void fraction can be expressed by the drift flux model suggested by Zuber and Findlay[18]. According to this model, the weighted mean gas velocity, $\overline{V_G}$, is represented by

$$\overline{V_G} = \overline{V_{Gj}} + C_0\langle j\rangle \tag{7}$$

and the following expression for average void fraction, $\langle\alpha\rangle$, can be derived from Eq. (7) ;

$$\frac{\langle\beta\rangle}{\langle\alpha\rangle} = C_o = \overline{V_{Gj}} / \langle j\rangle \tag{8}$$

In Eqs. (7) and (8), $\overline{V_{Gj}}$ is the weighted mean drift velocity, C_o is the void distribution parameter, $\langle\beta\rangle$ is the flowing volumetric concentration, and $\langle j\rangle$ is the area averaged superficial velocity of the mixture. These quantities are defined as follows;

$$\langle j\rangle = \langle j_L\rangle + \langle j_G\rangle \tag{9}$$

$$\overline{V_{Gj}} = \frac{\langle \alpha V_{Gj}\rangle}{\langle \alpha\rangle} \tag{10}$$

$$C_o = \frac{\langle \alpha j\rangle}{\langle \alpha\rangle\langle j\rangle} \tag{11}$$

$$\langle \beta\rangle = \frac{\langle j_G\rangle}{\langle j\rangle} \tag{12}$$

C_o and $\overline{V_{Gj}}$ are called drift flux parameters and take into account the effect of nonuniform concentration profile and the effect of the local relative velocity, respectively.

The drift flux model presentation of present data is illustrated in Figure 17 where $\langle j_L\rangle$ and channel inclination are treated as parameters. From this figure it can be noted that a linear relationship between $\overline{V_G}$ and $\langle j\rangle$ exists for the given value of $\langle j_L\rangle$. However effect of the liquid flow can be found irrespective of channel inclination.

On the other hand, the calculated values of $\overline{V_{Gj}}$ and $\langle j\rangle$ using the profiles of local void fraction and velocities are sufficiently small when compared with those of C_o, i.e. the absolute values ofboldoverline $\overline{V_{Gj}}$($\langle j\rangle C_o$) lies between 0.003 and

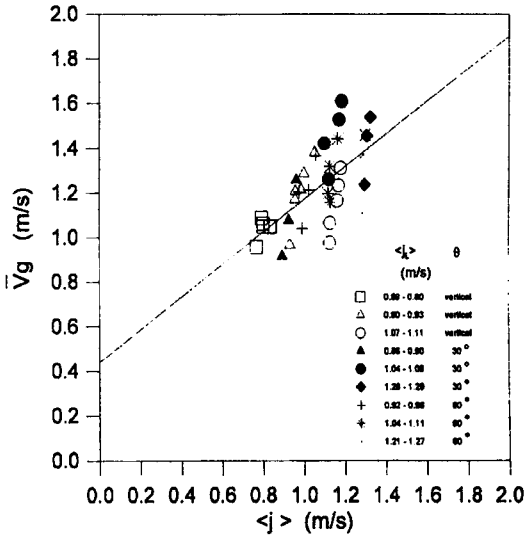

Fig. 17. Drift Flux Representation of Present Data

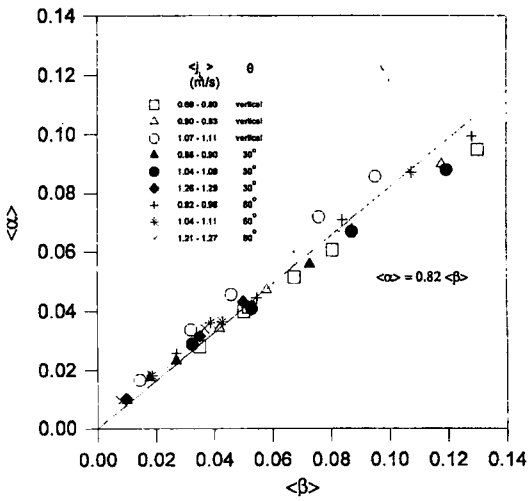

Fig. 18. $\langle\alpha\rangle-\langle\beta\rangle$ Representation of Present Data

0.166. This fact implies that the effect of the local relative velocity on the average void fraction is negligible when compared with the effect of nonuniform concentration distributions. So, the second term on the right hand side of Eq. (8) can

be neglected, and another plane, i.e. $\langle\alpha\rangle$-$\langle\beta\rangle$ plane is suggested to correlate the average void fraction. The data represented by the $\langle\alpha\rangle$-$\langle\beta\rangle$ plane are shown in Figure 18. By comparing Figures 17 and 18, it can be seen that $\langle\alpha\rangle$-$\langle\beta\rangle$ plane is superior because it correlates the data very well for the entire data range. This is not the case for the $\overline{V_G}$-<j> plane. Figure 17 indicates that the slope of solid line is 0.82 independent of the liquid flow rate and channel inclination, and the average void fraction can be expressed as follows;

$$\langle\alpha\rangle = 0.82\ \langle\beta\rangle \tag{13}$$

Eq.(13) predicts the average void fraction within a mean deviation of bold$\pm$9.5 %. Although Eq.(13) shows that the local relative velocity effect is negligible and thus the average void fraction in inclined subcooled boiling can be expressed in terms of flowing volumetric concentration irrespective of channel inclination, the data range was limited to low flow and low pressure subcooled boiling in annulus channel. So, further verification works need.

5. Summary and Conclusions

The internal flow structure of subcooled boiling in inclined annulus was investigated experimentally. The local two-phase flow parameters were measured by two-conductivity probe and Pitot tube. Major findings based on these measurements can be summarized as follows;

(1) The distribution of local void fraction in inclined channel is strongly influenced by the angle of inclination. As channel inclines toward the horizontal direction, the buoyancy provokes the migration of vapor bubbles toward the upper part of the cross section and the void fraction distribution becomes non-symmetric about the channel axis. Location of maximum void fraction moves toward channel center as average void fraction or inclination increases.

(2) The local vapor bubble frequency generally decreases from the heating surface to the outer wall over the entire cross section, irrespective of channel inclination. As channel inclination angle increases, the local chord length becomes large in the upper part of the cross section due to the bubble coalescence, and flow pattern transition to slug flow is observed depending on the flow condition.

(3) The local vapor bubble velocity in inclined channel generally increases as moving toward the upper part of the cross section due to the increase of bubble size. However, the effect of inclination is mitigated as the liquid flow rate increases. The liquid velocity profile in the most upper part of cross section is not parabolic, but gradually increases as moving toward the outer wall.

(4) For vertical channel, the increase of local IAC is mainly due to the increase of local bubble frequency. But the IAC in inclined channel is affected by bubble size.

(5) For correlating the present data, $\langle\alpha\rangle$-$\langle\beta\rangle$ Plane representation of the average void fraction is more appropriate than the drift flux representation.

Nomenclature

a_i : interfacial area concentration
C_o : void distribution parameter
D_h : hydraulic diameter
d_{sm} : Sauter mean diameter
j : superficial velocity of mixture
j_L : liquid superficial velocity
j_G : vapor superficial velocity
L : channel length

n_i : surface unit normal vector of interface.
N_t : bubble numbers per second
N_{szj} : number of bubbles having the velocity of v_{szj}
Δp : dynamic pressure measured by the Pitot tube
R_{inner} : radius of heating rod
R_{outer} : radius of channel
r : radial position
T : sampling time
Δt : time delay
$\overline{V_G}$: weighted mean gas velocity
V_G : vapor bubble velocity
V_L : liquid velocity
$\overline{V_{Gj}}$: weighted mean drift velocity
v_i : bubble interface velocity
v_{sz} : mean of v_{szj}
v_{szj} : velocity measured by two-conductivity probe
Δ_z : distance between two probe tips of two-conductivity probe
α : void fraction
α_o : the angle between the bubble velocity and the mean flow direction,
β : flowing volumetric concentration
ρ_L : liquid density
$<\Phi>$: area averaged value of quantity Φ

References

1. Barnea, D., Shoham, O., Taitel, Y and Dukler, A. E., "Flow Pattern Transition for Gas-Liquid Flow in Horizontal and Inclined Pipes - Comparison of Experimental Data with Theory," Int. J. Multiphase Flow, Vol. 6, pp. 217-225 (1980).
2. Barnea, D., Shoham, O., Taitel, Y and Dukler, A. E., "Gas Liquid Flow in Inclined Tubes : Flow Pattern Transitions for Upward Flow," Chemical Engineering Science, Vol. 40, pp 131-136 (1985).
3. Weisman, J. and Kang, S. Y., "Flow Pattern Transitions in Vertical and Upwardly Inclined Lines," Int. J. Multiphase Flow, Vol. 7, pp. 271-291 (1981).
4. Spedding, P. L., Chen, J.J.J. and Nguyen, V. T., "Pressure Drop in Two Phase Gas-Liquid Flow in Inclined Pipes," Int. J. Multiphase Flow, Vol. 8, No. 4, pp. 407-431 (1982).
5. Stanislav, J. F., Kokal, S. and Nicholson, M. K., "Intermittent Gas-Liquid Flow in Upward Inclined Pipes," Int. J. Multiphase Flow, Vol. 12, No. 3, pp. 325-335 (1986).
6. Spindler, K., "Void Fraction Distribution in Two Phase Gas Liquid Flow in Inclined Pipes," Proc. the Tenth International Heat Transfer Conference, Brighton, UK, Vol. 6, pp. 265-270 (1994).
7. Fedorov, M.V. and Klimenko, V.V., "The effect of Orientation of a Channel on Heat Transfer with Forced Two Phase Flow of Nitrogen,", Thermal Engineering, Vol. 35 (1988).
8. Neal, L.G. and Bankoff, S.G., "A High Resolution Resistivity Probe for Void Fraction Measurements in Air-Water Flow", AIChE J. pp. 490-494 (1963).
9. Serizawa, A., Kataoka, I. and Michiyoshi, I., "Turbulence Structure of Air-Water Bubbly Flows," Int. J. Multiphase Flow, Vol. 2, No. 4, pp. 221-233 (1975).
10. Welle, R.V., "Void Fraction, Bubble Velocity and Bubble Size in Two-Phase Flow," Int. J. Multiphase Flow, Vol. 11, No. 3, pp. 317-345 (1985).
11. Kocamustafaogullari, G. and Wang, Z., "An Experimental Study on Local Interfacial Parameters in a Horizontal Bubbly Two-Phase Flow," Int. J. Multiphase Flow, Vol. 17, No. 5, pp. 553-572 (1991).
12. Yun, B.J., Song, C.H., Sim, S.K., Chung, M. K. and Park, G.C., "Measurements of Local Two-Phase Flow Parameters in a Boiling Flow Channel," OECD/CSNI Special Meeting on Advanced Instrumentation and Measurement

Techniques, Santa Barbara (1997).

13. Ishii, M., "Thermo-Fluid Dynamic Theory of Two-Phase Flow," Eyrolles, Paris (1975).
14. Kataoka, I., Ishii, M. and Serizawa, A., "Local Formulation and Measurements of Interfacial Area Concentration In Two-Phase Flow," Int. J. Multiphase Flow, Vol. 12, No. 4, pp. 505-529 (1986).
15. Kataoka, I. and Serizawa, A., "Interfacial Area Concentration in Bubbly Flow," Nuclear Engineering and Design, Vol. 120, pp. 163-180 (1990).
16. Kataoka, I., Ishii, M. and Serizawa, A., "Sensitivity Analysis of Bubble Size and Probe Geometry on the Measurements of Interfacial Area Concentration in Gas-Liquid Two-Phase Flow," Nuclear Engineering and Design, Vol. 146, pp. 53-70 (1994).
17. Reimann, J., Kusterer, H. and Jhon, H., "Two Phase Mass Flow Rate Measurements with Pitot Tube and Density Measurements,", Measuring Techniques in Gas-Liquid Two-Phase Flows, Symposium, Nancy, France, July 5-8 (1983).
18. Zuber, N. and Findlay, J. A., "Average Volumetric Concentration in Two-Phase Flow Systems," J. Heat Transfer, November, pp, 453-468 (1965).